Inorganic Chemistry

pubs.acs.org/IC Article

Insights into the Synergistic Promotion Effect of Cu and W Modification on the Catalytic Performance of α-Fe_2O_3 for NH_3-SCR of NO_x

Qianni Cheng, Wanting Yan, Yirui Yang, Wang Song, Pengkai Jin, Chengyan Ge, Kaili Ma, Wei Tan,* Jingfang Sun,* and Lin Dong

Cite This: *Inorg. Chem.* 2025, 64, 9798−9806 Read Online

ACCESS | Metrics & More | Article Recommendations | Supporting Information

ABSTRACT: A dual-element modification strategy was proposed to promote the catalytic performance of the α-Fe_2O_3 catalyst for the selective catalytic reduction of NO_x by NH_3 (NH_3-SCR of NO_x) at both low and high temperatures. By optimizing the loading amount of CuO (4 wt %) and WO_3 (5 wt %), a wide operating temperature window (150−350 °C) was achieved on the modified α-Fe_2O_3 catalyst ($W_5/Cu_4/Fe$). Further characterizations revealed that the enhanced low-temperature activity could be attributed to the improved redox performance of α-Fe_2O_3 through CuO modification, while the superior high-temperature activity was primarily ascribed to the enhanced surface acidity induced by WO_3 modification. The synergistic effect of CuO and WO_3 modifications facilitated the NH_3-SCR reaction on the modified α-Fe_2O_3 catalysts to efficiently proceed through the Eley−Rideal (E−R) mechanism pathway. This provided compelling evidence that the catalytic performance of NH_3-SCR catalysts at different temperatures was dominantly governed by distinct factors (e.g., redox property and surface acidity), offering valuable insights for the rational design of robust catalysts for NO_x abatement.

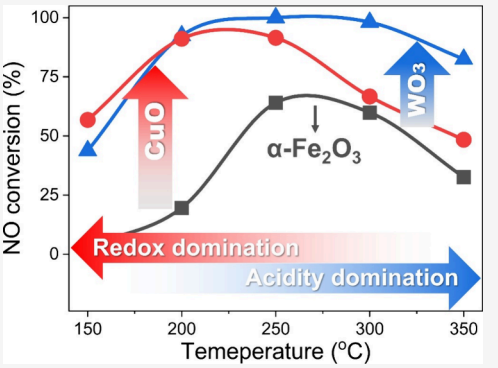

Downloaded via NANJING UNIV on May 21, 2025 at 08:24:23 (UTC).
See https://pubs.acs.org/sharingguidelines for options on how to legitimately share published articles.

1. INTRODUCTION

For decades, nitrogen oxides (NO_x) have been recognized as one of the most important air pollutants and have given rise to hosts of environmental issues, including acid rain, photochemical smog, and ozone layer depletion.[1−3] However, due to the complexity and variability of denitrification conditions in different sectors, the current selective catalytic reduction of NO_x by NH_3 (NH_3-SCR of NO_x) technology still faced challenges.[4−7] In addition to the increasing demand for low-temperature denitrification in various nonelectric industries, a large number of electric power industries also raised new denitrification requirements. For instance, during the processes of peak shaving and voltage regulation, efficient NO_x elimination should be realized under a full operating temperature window (150−350 °C), which exceeded the capabilities of commercial V_2O_5-$WO_3(MoO_3)/TiO_2$ catalysts. Therefore, the development of NH_3-SCR catalysts with excellent catalytic performance across a broad temperature window is on the horizon.

Fe-based catalysts have been widely studied due to their excellent redox properties, abundant reserves, and environmental friendliness. Hence, FeO_x after appropriate modifications, such as Fe-M-O_x (M = Ce,[8] Mn,[9] Co,[10] *etc.*), have been developed and applied for NH_3-SCR of NO_x. However, the simultaneous enhancement of catalytic activity at both high and low temperatures remains a significant challenge for Fe-based catalysts, and many efforts have been devoted to further widening the operating temperature window of Fe-based catalysts. For example, Chen et al. deposited CeO_2 onto the surface of Fe_2O_3, and the obtained Ce-Fe catalyst exhibited high NO conversion (>80%) within a wide range of 250−350 °C. However, NO conversion on the Ce-Fe catalyst was still lower than 50% below 200 °C.[11] Moreover, although the $FeMnO_x$ catalyst developed by Zhang et al. showed superior NH_3-SCR activity at low temperatures (80−210 °C), it suffered from a significant decrease in the NO conversion at high temperatures due to the overoxidation of NH_3.[12] That is, modifying FeO_x materials with a single element hardly simultaneously promoted the catalytic performance at low and high temperatures. Based on the consensus that the NH_3-SCR activity at different temperatures was governed by distinct factors (e.g., redox property and surface acidity),[13−16] it was inferred that multielement modification might be a promising

Received: March 6, 2025
Revised: April 17, 2025
Accepted: April 24, 2025
Published: May 6, 2025

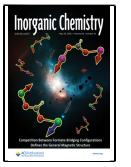

© 2025 American Chemical Society

https://doi.org/10.1021/acs.inorgchem.5c01039
Inorg. Chem. 2025, 64, 9798−9806

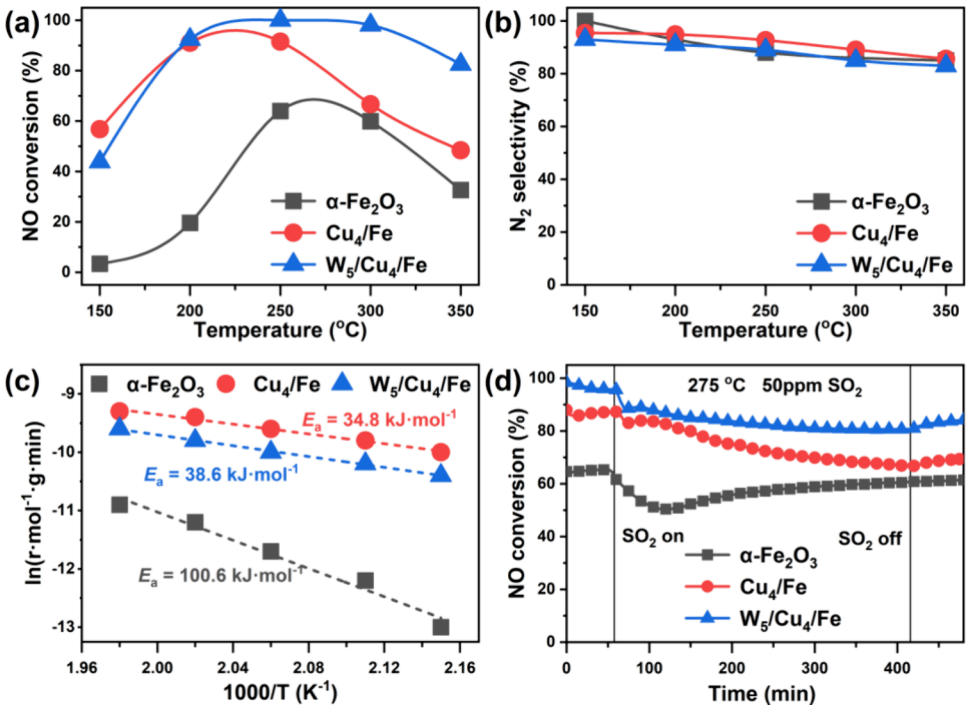

Figure 1. (a) NO conversion and (b) N_2 selectivity on α-Fe_2O_3, Cu_4/Fe, and W_5/Cu_4/Fe in the NH_3-SCR reaction. (c) Arrhenius plot and apparent activation energy (E_a) for α-Fe_2O_3, Cu_4/Fe, and W_5/Cu_4/Fe. (d) NO conversion on α-Fe_2O_3, Cu_4/Fe, and W_5/Cu_4/Fe in the NH_3-SCR reaction with the addition of SO_2 to the feed gas. Reaction conditions: [NH_3] = [NO] = 500 ppm, [O_2] = 4 vol %, [H_2O] = 5 vol % (when used), [SO_2] = 50 ppm (when used), N_2 balance, and WHSV = 60,000 mL·g^{-1}·h^{-1}.

strategy for broadening the operating temperature window of Fe-based NH_3-SCR catalysts.

CuO is a common reactive component in catalysts, which played a significant role in enhancing the redox performance of catalysts and remarkably boosting their low-temperature activity.[17−20] Dong et al. prepared a Cu-doped Fe_2O_3 catalyst, which demonstrated outstanding low-temperature performance, high N_2 selectivity, as well as excellent water and sulfur resistance in the NH_3-SCR reaction.[17] Xiong et al. also reported that the doping of Cu could increase the ratio of active Mn^{4+} in Mn_3O_4 spinel, thereby boosting its NH_3-SCR activity at low temperatures.[21] Moreover, the introduction of acidic metal oxides (Nb_2O_5,[22] MoO_3,[23] WO_3,[24,25] *etc.*) was the most common and effective way to improve high-temperature activity. For example, Geng et al. discovered that the introduction of W could provide additional Brønsted and Lewis acid sites with higher strength for NH_3 adsorption at high temperatures and suppress the overoxidation of NH_3, thus achieving satisfactory high-temperature NH_3-SCR performance.[26]

Herein, based on the understanding of the nature of metal oxide catalysts and NH_3-SCR reaction mechanism, a two-element modification strategy was proposed to promote the catalytic performance of Fe_2O_3 at low and high temperatures simultaneously. Specifically, the Fe_2O_3 catalyst modified with CuO and WO_3 demonstrated outstanding catalytic activity and high N_2 selectivity within a wide temperature range of 150−350 °C. In addition, it was elucidated that Cu modification improving the redox performance of Fe_2O_3 accounted for the boosted low-temperature activity, whereas W modification enhancing the surface acidity of Fe_2O_3 contributed to the improved high-temperature activity. This work is expected to provide insights into achieving a balance between redox and acidity for the design of efficient NH_3-SCR catalysts with wide operating temperature windows, thereby benefiting the environmental catalysis community.

2. EXPERIMENTAL SECTION

2.1. Catalyst Preparation. The α-Fe_2O_3 support was prepared by the ultrasonic-assisted coprecipitation method. Certain amounts of $FeSO_4·7H_2O$ (25 mmol) and $FeCl_3·6H_2O$ (50 mmol) were used as precursors and dissolved in deionized water (250 mL). Ammonia was added dropwise to the mixed solution until the pH reached 8.5 under vigorous stirring, and the stirring was continued for 2 h. Then the mixed solution was placed in an ultrasonic cleaner and sonicated for 2 h. The obtained sediment was washed with deionized water five times and ethanol three times to remove the remaining chloride ions and sulfate species. Then, the obtained sample was dried at 100 °C overnight and calcined at 400 °C for 3 h in a muffle furnace.

A series of x wt % CuO/α-Fe_2O_3 (x = 1, 3, 4, 5, and 8) catalysts were prepared by the incipient wetness impregnation (IWI) method. CuO was deposited onto α-Fe_2O_3 first using $Cu(NO_3)_2·3H_2O$ dissolved in excess $NH_3·H_2O$ (25%) as the Cu precursor followed by calcination at 400 °C for 2 h (denoted as Cu_x/Fe).

The y wt % WO_3/Cu_4/Fe catalysts (y = 1, 3, 5, and 8) were prepared by the wetness impregnation method using the above-mentioned Cu_4/Fe as support and $(NH_4)_6H_2W_{12}O_{40}·5H_2O$ as WO_3 precursor. The calculated amount of the $(NH_4)_6H_2W_{12}O_{40}·5H_2O$ precursor was first dissolved into deionized water in the presence of $H_2C_2O_4·2H_2O$ with equal weight. Then, Cu_4/Fe powder was added to the solution under vigorous stirring. Afterward, excess water was removed in an oil bath at 100 °C. The resulting solid was dried at 100 °C overnight and then calcined at 500 °C for 3 h in air (denoted as W_y/Cu_4/Fe). As a reference catalyst, 5 wt % WO_3/α-Fe_2O_3 (W_5/Fe) was synthesized using the IWI method and the same calcination treatment as W_y/Cu_4/Fe.

All samples were pressed into pellets, crushed, and sieved to 40−60 mesh before catalytic performance evaluation.

https://doi.org/10.1021/acs.inorgchem.5c01039
Inorg. Chem. 2025, 64, 9798−9806

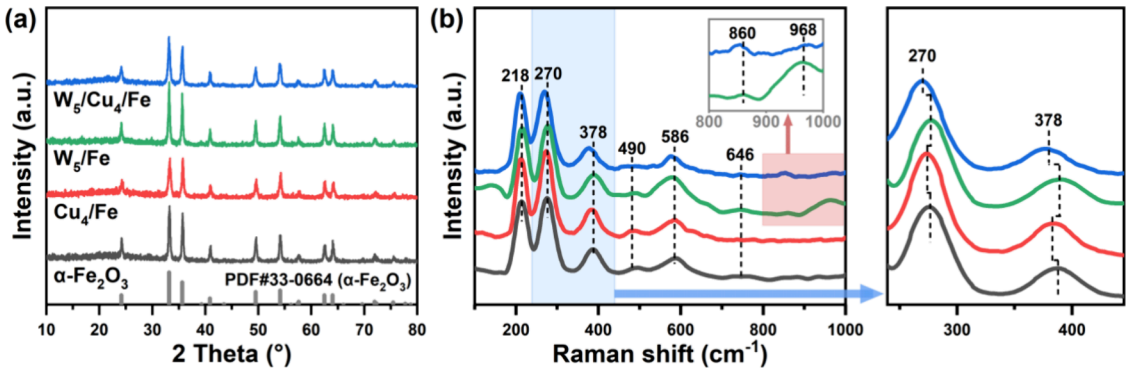

Figure 2. (a) The powder XRD patterns and (b) the Raman spectra of α-Fe_2O_3, Cu_4/Fe, W_5/Cu_4/Fe, and W_5/Fe.

Caution! *$NH_3{\cdot}H_2O$ (25%) is a liquid with a pungent odor and corrosive properties. All operations must be conducted in a fume hood.*

2.2. Catalyst Characterizations and Catalytic Performance Evaluation. A detailed description of characterization methods and performance measurements is provided in Supporting Information (Texts S1–S3).

3. RESULTS AND DISCUSSION

3.1. Catalytic Performance. It can be clearly observed from Figure 1a and Figure S1 that modification with CuO and WO_3 could significantly enhance the activity on α-Fe_2O_3. Specifically, after the addition of CuO, the low-temperature (≤250 °C) activity on α-Fe_2O_3 was improved notably, and 4 wt % CuO was the optimal loading amount. With the further deposition of WO_3 onto Cu_4/Fe, although the low-temperature activity even slightly decreased when the WO_3 loading reached 3 wt % or higher, the high-temperature activity on Cu_4/Fe also experienced a remarkable improvement, which increased from 40 to 80% at 350 °C. Considering the need to accommodate both low- and high-temperature activity, 5 wt % WO_3 should be the most appropriate loading. When compared with those recently reported Fe-based catalysts for the NH_3-SCR reaction, the W_5/Cu_4/Fe catalysts developed in this work still exhibited comparable catalytic performance (Table S1). Based on the well-established consensus that CuO modification and WO_3 modification were common and effective strategies to improve the redox performance and surface acidity of catalysts, respectively, it could be reasonably inferred that, correspondingly, these two properties served as the determining factors for low-temperature and high-temperature NH_3-SCR activity. Furthermore, a limited change in N_2 selectivity was observed after CuO and WO_3 modification, as shown in Figure 1b. To clarify the reasons for the decrease of the activity of α-Fe_2O_3, Cu_4/Fe and W_5/Cu_4/Fe at high temperatures, the concentration of NO_x (NO_2 and N_2O) in the outlet gas of the catalytic performance test was also measured and illustrated in Figure S2.

The apparent activation energy (E_a) of the NH_3-SCR reaction on α-Fe_2O_3, Cu_4/Fe, and W_5/Cu_4/Fe was also measured and is shown in Figure 1c (190–230 °C). After the introduction of CuO, E_a on α-Fe_2O_3 sharply decreased from 100.6 to 34.8 kJ·mol^{-1}, which meant that Cu modification could effectively lower the reaction energy barrier at low temperatures. Besides, E_a on W_5/Cu_4/Fe (38.6 kJ·mol^{-1}) was comparable to that on Cu_4/Fe, suggesting that W modification showed a limited negative impact on the low-temperature catalytic performance of Cu_4/Fe. The results of the reaction kinetics test further confirmed that the CuO modification could facilitate the proceeding of the NH_3-SCR reaction on α-Fe_2O_3.

Considering that SO_2 poisoning was one of the main obstacles to the real application of NH_3-SCR catalysts, the SO_2 resistance of the α-Fe_2O_3 before and after modification was tested, and the results are shown in Figure 1d. After the introduction of 50 ppm of SO_2 at 275 °C, the activity on α-Fe_2O_3 first decreased rapidly and then showed a slow upward trend after 1 h, which was due to the competitive adsorption between NO and SO_2 and the enhancement of surface acidity, respectively.[27,28] Since α-Fe_2O_3 showed outstanding SO_2 resistance, it is important to verify that CuO or WO_3 modification would enhance the catalytic performance of α-Fe_2O_3 without weakening the SO_2 resistance ability. The catalytic activity on Cu_4/Fe decreased sharply after the introduction of SO_2, which might be due to the stronger interaction of CuO species and SO_2.[29] It was notable that WO_3 modification retarded SO_2 poisoning effectively, indicating that α-Fe_2O_3 comodified by Cu and W could achieve superior NH_3-SCR activity and decent SO_2 resistance simultaneously. To better illustrate the inhibition effect of W modification on SO_2 poisoning, the concentration of SO_2 in the outlet gas of the SO_2 resistance test in the first 3 h was plotted (Figure S3). Although the addition of CuO would boost the SO_2 adsorption on Fe_2O_3, the introduction of WO_3 onto Cu_4/Fe could inhibit the adsorption of SO_2, which may delay the formation of sulfates. Additionally, our previous report indicated that dispersed MoO_3/WO_3 could shield CeO_2 from SO_2 poisoning due to the coordination of surface Ce sites by Mo–O/W–O.[30] In this work, the stronger interaction between WO_3 and the Fe/Cu sites might also suppress the adsorption of SO_2. It should be recognized that the SO_2 resistance ability of W_5/Cu_4/Fe still needs to be improved to meet the requirements of industrial application.

3.2. Structural Information. To reveal the reasons for the promotion effect of CuO and WO_3 modification, systematic characterizations were conducted to investigate the structure of the prepared catalysts. Besides, α-Fe_2O_3 modified with WO_3 (W_5/Fe) was also prepared as a reference catalyst to better demonstrate the possible interaction between CuO and WO_3.

According to the results of the N_2-physisorption experiment in Figure S4, CuO and/or WO_3 modification showed a limited impact on the specific surface area (S_{BET}), pore volume, and pore size of α-Fe_2O_3 (Table S2), which meant that the promotion of NH_3-SCR activity on α-Fe_2O_3 after CuO and/or WO_3 modification did not come from the change in its S_{BET} or pore structure. XRD analysis was conducted, and the results are displayed in Figure 2a. There was no obvious difference in

https://doi.org/10.1021/acs.inorgchem.5c01039
Inorg. Chem. 2025, 64, 9798–9806

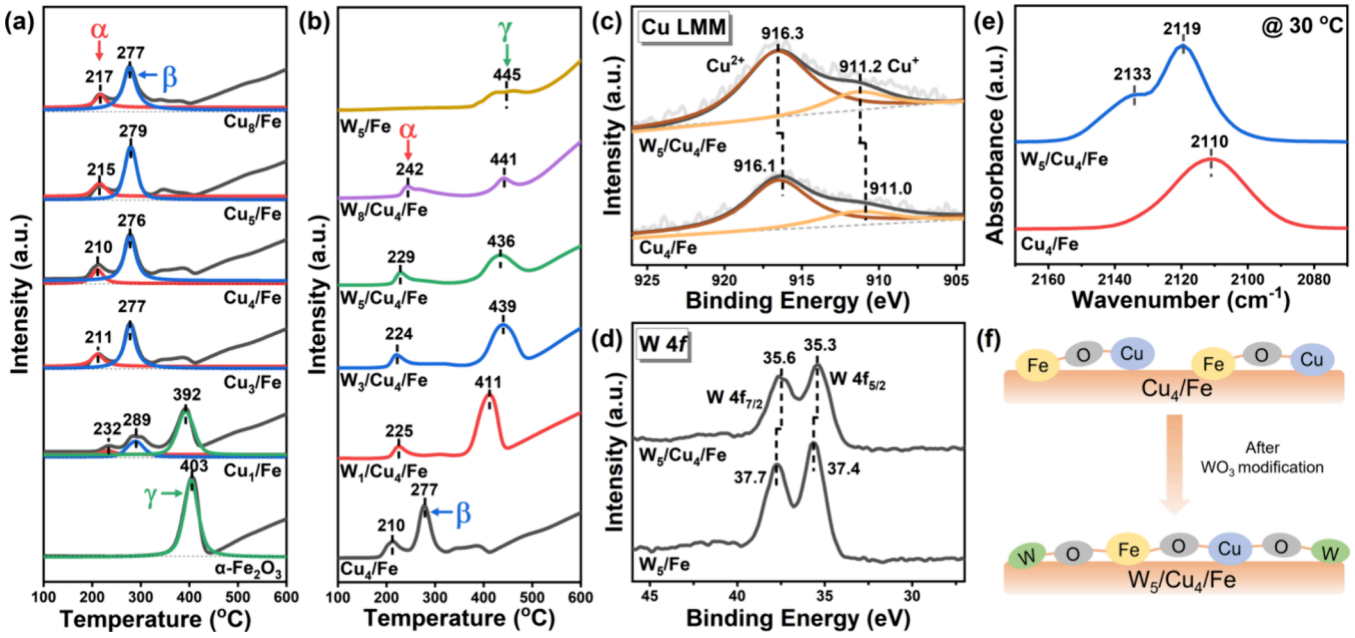

Figure 3. H_2-TPR profiles for (a) $Cu_{x/Fe}$ *and (b)* $W_{y/Cu_4/Fe}$. *XPS results of (c) Cu LMM and (d) W 4f for the prepared catalysts. (e) In situ DRIFTS of CO adsorption on* Cu_4/Fe *and* $W_5/Cu_4/Fe$ *catalysts. (f) Surface structural models of* Cu_4/Fe *and* $W_5/Cu_4/Fe$ *catalysts.*

the diffraction peaks of hematite α-Fe_2O_3 (JCPDS no. 33-0664) before and after CuO and WO_3 species modification, indicating that the bulk structure of α-Fe_2O_3 did not change. In addition, no diffraction peak attributed to CuO and WO_3 could be observed in all samples, suggesting that CuO and WO_3 species were highly dispersed or existed as small clusters under the limit of detection.

To further clarify the dispersion state of WO_3 and CuO, the TEM images and corresponding EDS-mapping images of the $W_5/Cu_4/Fe$ catalyst were recorded. As shown in Figure S5a, the $W_5/Cu_4/Fe$ catalyst was in the form of irregular nanoparticles. According to the EDS-mapping results shown in Figure S5b, CuO and WO_3 were evenly dispersed, and the distribution of Cu and W was closely associated with the distribution of Fe on the $W_5/Cu_4/Fe$ catalyst. The above results suggested that CuO and WO_3 were highly dispersed on α-Fe_2O_3, which was consistent with the XRD results. The Raman spectra of α-Fe_2O_3, Cu_4/Fe, $W_5/Cu_4/Fe$, and W_5/Fe catalysts are exhibited in Figure 2b. The characteristic bands at 218 (A_{1g}), 270 (E_g), 378 (E_g), 490 (A_{1g}), 586 (E_g), and 664 cm^{-1} (E_g) agreed well with the Raman active modes of α-Fe_2O_3.[31,32] No obvious peak corresponding to CuO was observed on the Cu_4/Fe catalyst, confirming the high dispersion of Cu species. However, after the introduction of the WO_3, new peaks at 860 and 968 cm^{-1} appeared on $W_5/Cu_4/Fe$ and W_5/Fe, which could be attributed to the stretching vibration of W−O−W and W═O structures within the highly dispersed polytungstate species,[33−35] respectively. Based on this, WO_3 configuration on $W_5/Cu_4/Fe$ was proposed (Figure S6).[34] In addition, compared to Cu_4/Fe and W_5/Fe, the peaks centered at 270 and 378 cm^{-1} related to the bending vibrations of Fe−O−Fe bonds on $W_5/Cu_4/Fe$ moved significantly toward lower Raman shift (Figure 2b), indicating the existence of strong interaction between WO_3/CuO with Fe_2O_3.[36]

3.3. Redox Properties and Surface Chemical States.

3.3.1. Redox Properties. Considering that the redox properties of catalysts were crucial for their catalytic performance in the NH_3-SCR reaction, H_2-TPR measurement was conducted. As shown in Figure 3a, the peak at 403 °C on pure α-Fe_2O_3 (denoted as the γ peak) was attributed to the reduced peak of Fe_2O_3 to Fe_3O_4.[37,38] After the introduction of Cu species, two new peaks appeared at around 200 °C. The peak at relatively lower temperature was attributed to the highly dispersed CuO species (denoted as the α peak). The peak at higher temperature was related to the reduction of Fe_2O_3 to Fe_3O_4 due to the H_2 spillover (denoted as the β peak). It could be inferred that the existence of highly dispersed CuO species and Cu−O−Fe interface significantly improved the low-temperature redox capability.[39] In addition, with the increase of CuO loading, peak α first gradually shifted to lower temperatures (from 232 to 210 °C) and then shifted to higher temperatures (from 210 to 217 °C) when the CuO loading exceeded 4 wt %. Therefore, it can be speculated that a CuO monolayer or small CuO clusters were formed on the surface of Cu_4/Fe, and higher loading of CuO would lead to the formation of agglomerated CuO species. These results indicated that the optimal CuO loading on α-Fe_2O_3 was 4 wt % for the improvement of redox performance.

H_2-TPR profiles for W_5/Fe and $W_y/Cu_4/Fe$ catalysts were also collected to investigate the impact of W modification on the redox property of Cu_4/Fe (Figure 3b). It was interesting to observe that the impregnation of WO_3 onto α-Fe_2O_3 led to a significant decrease in the intensity of peak γ, suggesting that the interaction between W and α-Fe_2O_3 could weaken the redox capability of α-Fe_2O_3. For $W_y/Cu_4/Fe$ catalysts, the loading of WO_3 resulted in the shift of peak α to higher temperatures, indicating the formation of a W−O−Cu interaction. Besides, the absence of peak β on $W_y/Cu_4/Fe$ could result from the inferior reducibility of the newly formed W−O−Fe structure even in the presence of H_2 spillover.[40] The reobserved peak γ on $W_y/Cu_4/Fe$ at high temperatures (*ca.* 420 °C) could be attributed to the reduction of the W−O−Fe structure. The above results indicated that the interaction between W and Cu would weaken the redox performance of Cu_4/Fe and Fe_2O_3.

To further clarify the impact of Cu and W modification on the activation of reactant molecules (NH_3 and NO) on α-Fe_2O_3, NH_3 and NO oxidation activity on the prepared

https://doi.org/10.1021/acs.inorgchem.5c01039
Inorg. Chem. 2025, 64, 9798−9806

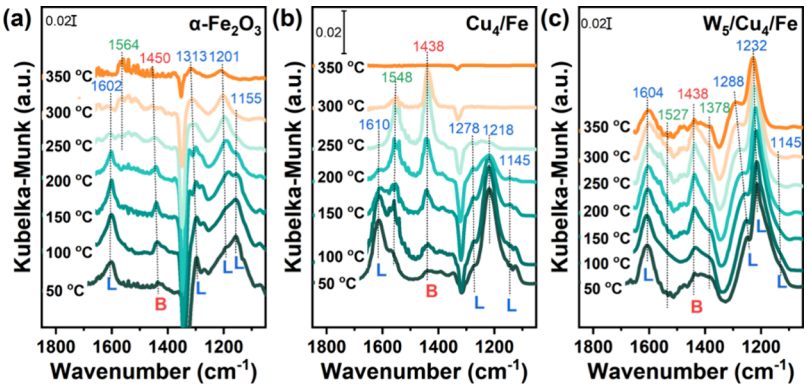

Figure 4. *In situ* DRIFTS of NH_3 adsorption on (a) α-Fe_2O_3, (b) Cu_4/Fe, and (c) W_5/Cu_4/Fe.

catalysts was evaluated (Figure S7). It was found that CuO modification could remarkably improve NH_3 and NO oxidation activity on Fe_2O_3, indicating that Cu sites could promote the activation of NH_3 and NO. However, the introduction of WO_3 species would significantly suppress the oxidation of NH_3 and NO on the Cu_4/Fe catalyst, matching well with the results of H_2-TPR that the interaction between W and Cu would weaken the redox performance of Cu_4/Fe and Fe_2O_3.

3.3.2. Surface Chemical States. To investigate the surface chemical states of the catalysts, XPS experiments were conducted (Figure 3c,d and Figure S8). For Cu LMM XPS, the peaks near 916 and 911 eV were attributed to Cu^{2+} and Cu^+ of Cu $2p_{3/2}$, respectively (Figure 3c).[41] For W 4*f* XPS, the peak of W $4f_{7/2}$ around 37 eV and W$4f_{5/2}$ around 35 eV were observed (Figure 3d).[42] When using Cu_4/Fe and W_5/Fe as references, Cu $2p_{3/2}$ XPS of W_5/Cu_4/Fe shifted toward higher binding energy, while W 4*f* XPS of W_5/Cu_4/Fe shifted toward lower binding energy, indicating a strong electronic interaction between W and Cu through the W−O−Cu bond, which was consistent with H_2-TPR results. In addition, as shown in Table S3, the $Cu^+/(Cu^+ + Cu^{2+})$ ratio on Cu_4/Fe (29.1%) was found to decrease after the introduction of W species (22.8%), suggesting the reduced electron cloud density of Cu atom due to the electron transfer from Cu to W. Just as reported by Qi et al. that the presence of Cu^+ was beneficial to the redox cycle of $Cu^{2+} + Fe^{2+} \leftrightarrow Cu^+ + Fe^{3+}$,[19] the introduction of WO_3 species would weaken the redox capability of Cu_4/Fe, thus slightly lowering its low-temperature activity (Figure 1a).

In situ DRIFTS of CO adsorption was also employed to investigate the interaction between Cu and W (Figure 3e). For Cu_4/Fe, the symmetric IR band at 2110 cm^{-1} could be attributed to CO adsorbed on Cu^+ sites ($(CO)_n$@Cu^+).[43] After the deposition of WO_3, a blue shift of the CO IR band was observed on W_5/Cu_4/Fe, which could be due to the electron-withdrawing inductive effect of the nearby W−O ligands through W−O−Cu interfaces,[44] further confirming the formation of strong interaction between W and Cu. In addition, the red shift of the CO IR band on W_5/Cu_4/Fe with the increase of exposure time indicated that Cu^{2+} that interacted with W would be slowly reduced by CO due to its relatively inferior reducibility (Figure S9).[45] *In situ* DRIFTS of CO adsorption experiments on W_y/Cu_4/Fe with different WO_3 loadings were also conducted (Figure S10). With the increase of WO_3 loadings from 3 to 8 wt %, a blue shift of the CO IR bands was observed, further confirming that the shift of the CO IR bands was related to the formation of the W−O−Cu structure and W−Cu interaction.

Based on the results of H_2-TPR, XPS, and *in situ* DRIFTS of CO adsorption, surface structural models of Cu_4/Fe and W_5/Cu_4/Fe were proposed (Figure 3f). On the surface of the Cu_4/Fe catalyst, the formation of the Cu−O−Fe structure drastically improved the redox performance of α-Fe_2O_3. When WO_3 was further introduced, the generation of strong interaction between WO_3 and Cu−O−Fe (W−O−Cu or W−O−Fe) resulted in a diminished redox capability.

3.4. Surface Adsorption Property. In addition to the redox property, the adsorption and activation abilities of the catalyst for reactants also play a vital role in the NH_3-SCR reaction. Therefore, the adsorption characteristics of NH_3/NO_x on the prepared catalysts were further investigated by TPD and *in situ* DRIFTS experiments.

3.4.1. Adsorbed NH_3 Species. We first carried out an NH_3-TPD test to determine the amount of acid sites on the catalyst surface, and the results are shown in Figure S11 and Table S4. After the introduction of CuO, the NH_3 adsorption amount was significantly reduced from 50 to 30 $\mu mol/g_{cat}$, suggesting the loss of acid sites because of the CuO modification.[46] Since Cu_4/Fe showed better low-temperature activity than α-Fe_2O_3, it could be inferred that the key factor determining the low-temperature NH_3-SCR performance of α-Fe_2O_3 was redox performance instead of surface acidity. The further loaded WO_3 species onto Cu_4/Fe were found to serve as strong acid sites, and the NH_3 adsorption amount increased from 30 to 60 $\mu mol/g_{cat}$, which should be the main reason for the promotion of NH_3-SCR activity at relatively high temperatures (>250 °C).

To further clarify the types of surface acid sites on the prepared catalysts, NH_3-DRIFTS experiments were conducted (Figure 4). As shown in Figure 4a, the intensive band at 1155, 1201, 1313, and 1602 cm^{-1} observed on α-Fe_2O_3 could be attributed to NH_3 adsorbed on Lewis acid sites (surface Fe ions),[47] while the weak band at ca. 1450 cm^{-1} was related to NH_4^+ species coordinated to Brønsted acid sites (surface Fe-OH sites).[24,48] After the modification of CuO, the coverage of Fe ions by Cu ions resulted in the appearance of a new intensive band at ca. 1218 cm^{-1}, which could be ascribed to NH_3 adsorbed on Cu ions serving as the Lewis acid site. With the further impregnation of WO_3, a new intensive band at ca. 1288 cm^{-1} emerged, which could be assigned to NH_3 adsorbed on WO_3 species (Lewis acid sites).[43] In addition, the band attributed to NH_3 adsorbed on Brønsted acid sites was also enhanced on WO_3-modified catalysts because the W−OH

https://doi.org/10.1021/acs.inorgchem.5c01039
Inorg. Chem. 2025, 64, 9798−9806

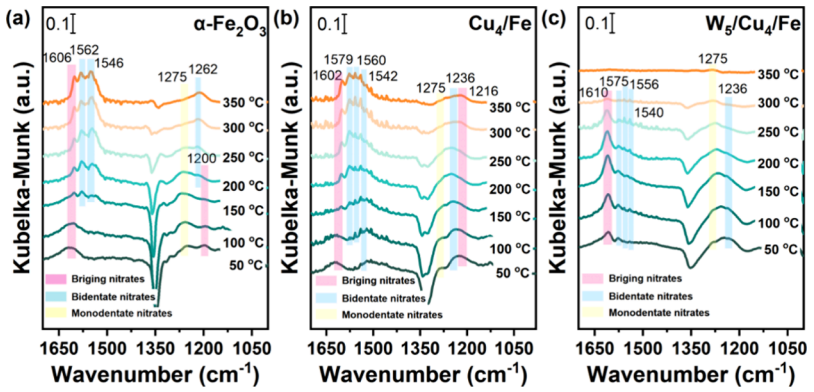

Figure 5. *In situ* DRIFTS of NO + O_2 adsorption on (a) α-Fe_2O_3, (b) Cu_4/Fe, and (c) W_5/Cu_4/Fe.

species could also act as Brønsted acid sites.[24] The significant shift of IR bands attributed to NH_3 adsorbed on Lewis acid sites matches well with the surface modification process. After the introduction of CuO, the decrease in the intensity of the IR bands attributed to NH_3 adsorbed on acid sites indicated that the acidity of the catalyst has been weakened, which is consistent with the NH_3-TPD results. In addition, the strength of the Lewis acid also increased after WO_3 modification. The results indicated that the surface loading of WO_3 enhanced the Lewis and Brønsted acid sites to provide abundant acidity for the catalyst, which was more conducive to the adsorption of NH_3. In addition to Lewis and Brønsted acid species, an IR peak at 1564 cm^{-1} attributed to nitrate species was observed on α-Fe_2O_3, which was due to the oxidation of adsorbed NH_3 species by surface active oxygen species.[49,50] Nitrate species generated by NH_3 oxidation were also observed on Cu_4/Fe (1548 cm^{-1}) and W_5/Cu_4/Fe (1378 and 1527 cm^{-1}). Furthermore, as the temperature increased, the acidic strength of all catalysts decreased. For Cu_4/Fe, its Lewis acid almost completely disappeared above 300 °C, while the acidity of W_5/Cu_4/Fe still retained strong acidity at 350 °C compared with α-Fe_2O_3 and Cu_4/Fe. It can be inferred that the significant increase in acidity after WO_3 modification was the key factor for the increase of activity in the high temperature.

By integrating the findings from the catalytic performance evaluation, H_2-TPR, NH_3-TPD, and NH_3-DRIFTS, it could be postulated that the improvement in redox capacity predominantly enhanced the low-temperature catalytic performance, while the augmentation of surface acidity primarily contributed to the high-temperature activity of the α-Fe_2O_3 catalyst.

3.4.2. Adsorbed NO_x Species. To reveal whether CuO and WO_3 modification would affect the adsorption of NO_x on α-Fe_2O_3, the NO + O_2-TPD test was first carried out. As shown in Figure S12 and Table S5, although CuO modification slightly promoted the adsorption of NO_x on Fe_2O_3 catalysts, further modification by WO_3 significantly suppressed the adsorption and oxidation of NO.

To further clarify the types of nitrates, *in situ* DRIFTS of NO + O_2 adsorption experiments was also carried out. As shown in Figure 5, the bands related to bridging bidentate nitrates (1606 and 1200 cm^{-1}), the chelating bidentate nitrates (1562, 1546, and 1262 cm^{-1}), and monodentate nitrates (1275 cm^{-1}) were observed.[51] After the introduction of CuO, the intensity of all bands increased significantly, which indicated that the CuO component was beneficial for promoting the adsorption and activation of nitrate species. After further loading of WO_3, the nitrate species on the surface of the W_5/Cu_4/Fe decreased significantly, and the bridging bidentate nitrates at 1216 cm^{-1} almost disappeared. The nitrates on the surfaces of W_5/Cu_4/Fe were mainly bridged nitrates at 1610 cm^{-1} chelating bidentate nitrates around 1556 and 1236 cm^{-1}.

3.5. Reaction Mechanism. In view of the alternations of NH_3/NO adsorption characteristics on α-Fe_2O_3 induced by CuO/WO_3 modification, *in situ* DRIFTS of surface reaction experiments were conducted to investigate the possible change in the reaction mechanism.

NO + O_2 was first introduced to catalysts with preadsorbed NH_3 to determine the reactivity of adsorbed NH_3 species (Figure 6). Upon the introduction of NO + O_2, the intensity of bands assigned to NH_3 on Lewis and Brønsted acid sites decreased rapidly on all catalysts, suggesting that the SCR reaction could proceed through the Eley−Rideal (E−R) mechanism efficiently. In addition, we calculated the peak

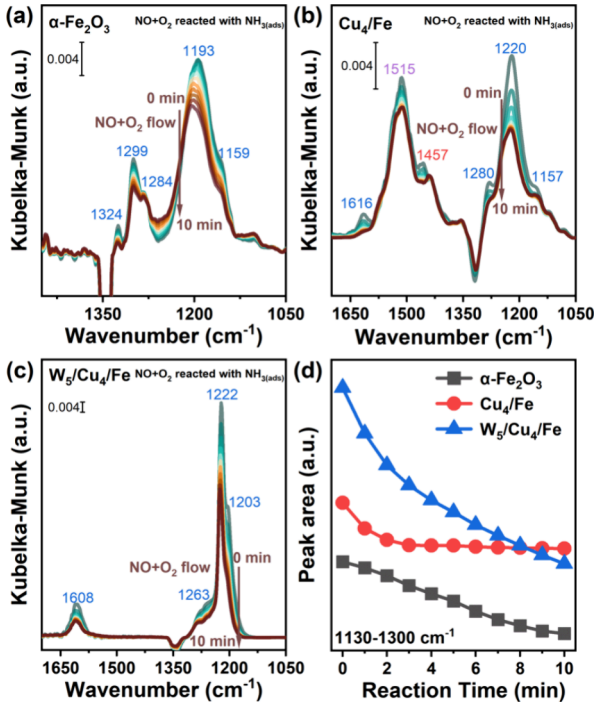

Figure 6. *In situ* DRIFTS of NO + O_2 reacting with preadsorbed NH_3 at 175 °C on (a) α-Fe_2O_3, (b) Cu_4/Fe, and (c) W_5/Cu_4/Fe and (d) the peak area of IR bands corresponding to NH_3 adsorbed on Lewis acid species as a function of reaction time (the bands marked in blue and red fonts represent Lewis acid and Brønsted acid, respectively).

https://doi.org/10.1021/acs.inorgchem.5c01039
Inorg. Chem. 2025, 64, 9798−9806

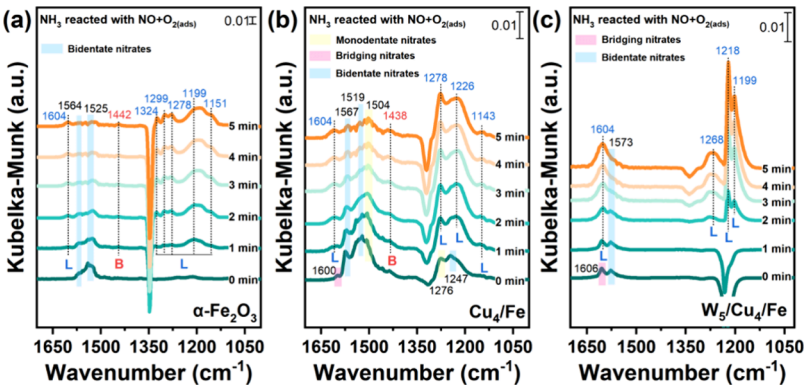

Figure 7. *In situ* DRIFTS of NH_3 reacting with preadsorbed NO + O_2 at 175 °C on (a) α-Fe_2O_3, (b) Cu_4/Fe, and (c) W_5/Cu_4/Fe.

area corresponding to the Lewis acid species as a function of reaction time, as shown in Figure 6d. Apparently, the consumption rate of L-NH_3 species on Cu_4/Fe and W_5/Cu_4/Fe was much higher than that on α-Fe_2O_3 in the first few seconds, indicating that CuO modification could benefit the adsorption and activation of NH_3, thus facilitating the reaction of NO and adsorbed NH_3. It is worth noting that the initial acid strength of W_5/Cu_4/Fe was significantly higher than that of α-Fe_2O_3 and Cu_4/Fe, indicating that the modification of WO_3 significantly enhanced the surface acidity of the catalysts. Combined with the results of H_2-TPR and NO+O_2-TPD, WO_3 modification would weaken the low-temperature redox performance of Cu_4/Fe and suppress the adsorption of NO_x, which might decrease the efficiency of NH_3 and NO activation. However, considering that the NH_3-SCR reaction on W_5/Cu_4/Fe mainly followed the E−R reaction pathway, as confirmed by the DRIFTS study, more acid sites introduced by WO_3 modification would facilitate the adsorption of more NH_3, thus compensating for the loss of low-temperature redox performance and NO_x adsorption.

To further evaluate the reactivity of adsorbed NO_x on the prepared catalysts, *in situ* DRIFTS of NH_3 reacting with preadsorbed NO_x experiments was also conducted (Figure 7). When NH_3 was introduced, chelating bidentate nitrates on α-Fe_2O_3 (1564 and 1525 cm^{-1}), Cu_4/Fe (1567 and 1519 cm^{-1}), and W_5/Cu_4/Fe (1573 cm^{-1}) were gradually depleted, and the bridging nitrates (1600 and 1606 cm^{-1}) on Cu_4/Fe and W_5/Cu_4/Fe were also consumed quickly. At the same time, IR bands attributed to NH_3 adsorbed on acid sites rapidly emerged on all of the catalysts. The results above showed that the NH_3-SCR reaction on α-Fe_2O_3, Cu_4/Fe, and W_5/Cu_4/Fe could also follow the Langmuir−Hinshelwood (L−H) mechanism. In general, there was no significant change in the trend of the L−H mechanism on them, so this was not the key mechanism that caused the difference in activity.

In short summary, the results of the DRIFTS study disclosed that the NH_3-SCR reaction on α-Fe_2O_3, Cu_4/Fe, and W_5/Cu_4/Fe followed both E−R and L−H mechanisms, and the superior NH_3-SCR activity on Cu_4/Fe and W_5/Cu_4/Fe was primarily attributed to the enhanced E−R reaction pathway. After CuO modification, the activation of NH_3 adsorbed on α-Fe_2O_3 was drastically promoted, thus benefiting the NH_3-SCR reaction through the E−R mechanism. Besides, strong acid sites on WO_3-modified catalysts could enable the NH_3-SCR reaction to advance efficiently at high temperatures through the E−R pathway. To better illustrate the promotion effect of CuO and WO_3 modification on the α-Fe_2O_3 catalyst, a scheme was proposed (Scheme 1).

Scheme 1. Scheme of the Enhanced E−R Reaction Pathway on the W_5/Cu_4/Fe Catalyst

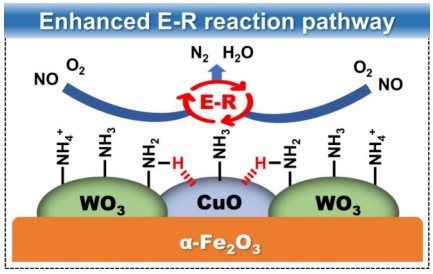

4. CONCLUSIONS

In this work, the catalytic performance of α-Fe_2O_3 catalysts in the NH_3-SCR reaction was significantly improved by CuO and WO_3 modification. The W_5/Cu_4/Fe catalyst with optimal loadings of CuO and WO_3 showed excellent NH_3-SCR reactivity over a wide temperature window (150−350 °C). CuO modification significantly improved the redox capability of α-Fe_2O_3, thereby benefiting from the increase in the low-temperature activity. In contrast, although further WO_3 even slightly diminished the redox capability of Cu_4/Fe, the enhanced surface acidity promoted the adsorption of NH_3 at high temperatures, consequently contributing to the improvement of high-temperature NH_3-SCR activity. The dual-element modification strategy proposed in this work provided a promising approach for the development of highly efficient catalysts, offering an optimal balance between low- and high-temperature catalytic activity.

■ ASSOCIATED CONTENT

Supporting Information

The Supporting Information is available free of charge at https://pubs.acs.org/doi/10.1021/acs.inorgchem.5c01039.

Details of catalyst characterizations and catalytic performance evaluation, NH_3-SCR activity, product distribution, SO_2 signal in the outlet gas of SO_2 resistance test, N_2-physisorption, TEM images, EDS-mapping images, WO_3 configuration, NH_3 oxidation activity, NO oxidation activity, XPS, CO-DRIFTS, NH_3-TPD, NO + O_2-TPD, and catalytic performance of recently reported Fe-based catalysts (PDF)

https://doi.org/10.1021/acs.inorgchem.5c01039
Inorg. Chem. 2025, 64, 9798−9806

AUTHOR INFORMATION

Corresponding Authors

Wei Tan − *State Key Laboratory of Pollution Control and Resource Reuse, School of Environment, Jiangsu Key Laboratory of Vehicle Emissions Control, Nanjing University, Nanjing 210023, P. R. China;* orcid.org/0000-0002-1481-9346; Email: tanwei@nju.edu.cn

Jingfang Sun − *Center of Modern Analysis, Nanjing University, Nanjing 210023, P. R. China;* orcid.org/0000-0003-1963-4874; Email: sunjf@nju.edu.cn

Authors

Qianni Cheng − *State Key Laboratory of Pollution Control and Resource Reuse, School of Environment, Jiangsu Key Laboratory of Vehicle Emissions Control, Nanjing University, Nanjing 210023, P. R. China*

Wanting Yan − *School of Chemistry and Chemical Engineering, Nanjing University, Nanjing 210023, P. R. China*

Yirui Yang − *State Key Laboratory of Pollution Control and Resource Reuse, School of Environment, Jiangsu Key Laboratory of Vehicle Emissions Control, Nanjing University, Nanjing 210023, P. R. China*

Wang Song − *School of Chemistry and Chemical Engineering, Nanjing University, Nanjing 210023, P. R. China*

Pengkai Jin − *State Key Laboratory of Pollution Control and Resource Reuse, School of Environment, Jiangsu Key Laboratory of Vehicle Emissions Control, Nanjing University, Nanjing 210023, P. R. China*

Chengyan Ge − *School of Chemistry and Chemical Engineering, Yancheng Institute of Technology, Yancheng 224051, P. R. China*

Kaili Ma − *Analysis and Testing Center, Southeast University, Nanjing 211189, China*

Lin Dong − *State Key Laboratory of Pollution Control and Resource Reuse, School of Environment, Jiangsu Key Laboratory of Vehicle Emissions Control and School of Chemistry and Chemical Engineering, Nanjing University, Nanjing 210023, P. R. China;* orcid.org/0000-0002-8393-6669

Complete contact information is available at: https://pubs.acs.org/10.1021/acs.inorgchem.5c01039

Notes

The authors declare no competing financial interest.

ACKNOWLEDGMENTS

J.S. acknowledges the support from the National Natural Science Foundation of China (22202100). W.T. acknowledges the support from the National Natural Science Foundation of China (22306090), Natural Science Foundation of Jiangsu Province (BK20230773), and Young Elite Scientists Sponsorship Program by CAST (YESS20230298). L.D. acknowledges the support from the National Natural Science Foundation of China (22272077) and Natural Science Foundation of Jiangsu Province (BK20231513). K.M. acknowledges the support from the National Natural Science Foundation of China (22402027).

REFERENCES

(1) Chen, W.; Zou, R.; Wang, X. Toward an Atomic-Level Understanding of the Catalytic Mechanism of Selective Catalytic Reduction of NO_x with NH_3. *ACS Catal.* **2022**, *12* (22), 14347−14375.

(2) Liu, J.; Burciaga, R.; Tang, S.; Ding, S.; Ran, H.; Zhao, W.; Wang, G.; Zhuang, Z.; Xie, L.; Lyu, Z.; Lin, Y.; Du, A.; Yuan, A.; Fu, J.; Song, B.; Zhu, J.; Sun, Z.; Jin, X.; Huo, Z.-Y.; Shen, B.; Shen, M.; Cao, Y.; Zhou, Y.; Jiang, Y.; Zhu, D.; Sun, M.; Wu, X.; Qin, C.; Jiang, Z.; Metin, O.; Thambiliyagodage, C. J.; Lv, J.-J.; Li, Q.; Wu, H.; Wu, Z.; Lam, J. C.-H.; Gao, G.; Li, C.; Luo, M.; Jiang, Y.; Wang, X.; Li, J.; Liu, M.; Lin, R.; Ren, H.; Han, B.; Jing, Y.; Zhu, W. Heterogeneous Catalysis for the Environment. *Innov. Mater.* **2024**, *2* (3), No. 100090.

(3) Zhang, N.; He, H.; Wang, D.; Li, Y. Challenges and Opportunities for Manganese Oxides in Low-Temperature Selective Catalytic Reduction of NO_x with NH_3: H_2O Resistance Ability. *J. Solid State Chem.* **2020**, *289*, No. 121464.

(4) Huang, Q.; Song, L.; He, H.; Qiu, W.; Su, Y. Effects of SO_2 Treatment of Commercial Catalysts on Selective Catalytic Reduction of NO_x by NH_3. *Chem. Res. Chin Univ.* **2016**, *32* (3), 414−417.

(5) Huang, X.; Zhang, G.; Lu, G.; Tang, Z. Recent Progress on Establishing Structure-Activity Relationship of Catalysts for Selective Catalytic Reduction (SCR) of NO_x with NH_3. *Catal. Surv. from Asia.* **2018**, *22* (1), 1−19.

(6) Xu, G.; Li, H.; Yu, Y.; He, H. Dynamic Change of Active Sites of Supported Vanadia Catalysts for Selective Catalytic Reduction of Nitrogen Oxides. *ENVIRON SCI TECHNOL.* **2022**, *56* (6), 3710−3718.

(7) Zhang, S.; Liu, Q.; Liu, Z.; Luo, C.; Song, W.; Chen, H.; Li, J.; Tan, W.; Gao, F.; Dong, L. Cu-SSZ-39@CeSi Core-Shell Catalyst: A High Sulfur Resistant Catalyst in NH_3-SCR Reaction. *J. Rare Earths.* **2025**, DOI: 10.1016/j.jre.2025.03.016.

(8) Chen, W.; Yang, S.; Liu, H.; Huang, F.; Shao, Q.; Liu, L.; Sun, J.; Sun, C.; Chen, D.; Dong, L. Single-Atom Ce-Modified α-Fe_2O_3 for Selective Catalytic Reduction of NO with NH_3. *ENVIRON SCI TECHNOL.* **2022**, *56* (14), 10442−10453.

(9) Mo, D.; Qin, Q.; Huang, C.; Tao, L.; Li, C.; Qiu, J.; Wang, J.; Han, X.; Gu, S.; Chen, Z.; Li, B.; Dong, L. Regulating the Distribution of Iron Active Sites on γ-Fe_2O_3 via Mn-Modified α-Fe_2O_3 for NH_3-SCR. *APPL CATAL B-ENVIRON.* **2024**, *349*, No. 123869.

(10) Shao, C. Z.; Liu, X. F.; Meng, D. M.; Xu, Q.; Guo, Y. L.; Guo, Y.; Zhan, W. C.; Wang, L.; Lu, G. Z. Catalytic Performance of Co-Fe Mixed Oxide for NH_3-SCR Reaction and the Promotional Role of Cobalt. *RSC Adv.* **2016**, *6* (70), 66169−66179.

(11) Chen, Y.; Zhang, Y.; Feng, X.; Li, J.; Liu, W.; Ren, S.; Yang, J.; Liu, Q. In Situ Deposition of 0D CeO_2 Quantum Dots on Fe_2O_3-Containing Solid Waste NH_3-SCR Catalyst: Enhancing Redox and NH_3 Adsorption Ability. *WASTE MANAGE* **2022**, *149*, 323−332.

(12) Zhang, X.; Wang, D.; Peng, J.; Lu, C.; Xu, L. Influence of Calcination Temperature on Structural Property of Mn Doped γ-Fe_2O_3 Catalysts and Low-Temperature SCR Activity. *J. Fuel Chem. Technol.* **2015**, *43* (2), 243−250.

(13) An, D.; Ji, J.; Cheng, Q.; Zhao, X.; Cai, Y.; Tan, W.; Tong, Q.; Ma, K.; Zou, W.; Sun, J.; Tang, C.; Dong, L. Facile H_2O-Contributed O_2 Activation Strategy over Mn-Based SCR Catalysts to Counteract SO_2 Poisoning. *ENVIRON SCI TECHNOL.* **2023**, *57* (39), 14737−14746.

(14) Hou, L.; Sun, X.; Li, J.; Lu, L.; Wang, T.; Wu, W. Denitrification Performance and Mechanism of NH3-SCR Rare Earth Tailings Catalyst Modified by Ce Combined with Mn. *Res. Chem. Intermed.* **2025**, *51* (2), 721−741.

(15) Ji, J.; Jing, M.; Wang, X.; Tan, W.; Guo, K.; Li, L.; Wang, X.; Song, W.; Cheng, L.; Sun, J.; Song, W.; Tang, C.; Liu, J.; Dong, L. Activating low-temperature NH_3-SCR catalyst by breaking the strong interface between acid and redox sites: A case of model $Ce_2(SO_4)_3$-CeO_2 study. *J. Catal.* **2021**, *399*, 212−223.

(16) Tan, W.; Wang, C.; Yu, S.; Li, Y.; Xie, S.; Gao, F.; Dong, L.; Liu, F. Revealing the Effect of Paired Redox-Acid Sites on Metal Oxide Catalysts for Efficient NO_x Removal by NH_3-SCR. *J. Hazard. Mater.* **2021**, *416*, No. 125826.

(17) Dong, S.; Wang, H.; Zhu, T.; Qu, Z. High-Performance Fe-Cu Composite Oxide for Selective Catalytic Reduction of NO_x with NH_3:

Driving of Cu on α-Fe_2O_3. *J. Environ. Chem. Eng.* **2022**, *10* (5), No. 108481.
(18) Guo, R.-T.; Zhen, W.-L.; Pan, W.-G.; Zhou, Y.; Hong, J.-N.; Xu, H.-J.; Jin, Q.; Ding, C.-G.; Guo, S.-Y. Effect of Cu Doping on the SCR Activity of CeO_2 Catalyst Prepared by Citric Acid Method. *J. Ind. and Eng. Chem.* **2014**, *20* (4), 1577−1580.
(19) Qi, L.; Sun, Z.; Tang, Q.; Wang, J.; Huang, T.; Sun, C.; Gao, F.; Tang, C.; Dong, L. Getting insight into the effect of CuO on red mud for the selective catalytic reduction of NO by NH_3. *J. Hazard. Mater.* **2020**, *396*, No. 122459.
(20) Wang, X.; Chi, R.; Gu, L.; Sun, L.; Liu, Y.; Wu, Z. Effect of Water Vapor on Low Temperature SCR Performances over Cu and Mn-Based Catalysts: A Comparison Study. *J. Rare Earths.* **2024**.
(21) Xiong, S.; Peng, Y.; Wang, D.; Huang, N.; Zhang, Q.; Yang, S.; Chen, J.; Li, J. The Role of the Cu Dopant on A Mn_3O_4 Spinel SCR Catalyst: Improvement of Low-Temperature Activity and Sulfur Resistance. *Chem. Eng. J.* **2020**, *387*, No. 124090.
(22) Zhang, W.; Shi, X.; Yan, Z.; Shan, Y.; Zhu, Y.; Yu, Y.; He, H. Design of High-Performance Iron-Niobium Composite Oxide Catalysts for NH_3-SCR: Insights into the Interaction between Fe and Nb. *ACS Catal.* **2021**, *11* (15), 9825−9836.
(23) Wang, J.; Xu, Z.; Zhao, W.; Li, X. Selective Catalytic Reduction of NO by NH_3 over MoO_3 Promoted Fe_2O_3 Catalyst. *Kinet. Catal.* **2018**, *59* (5), 628−634.
(24) Liu, F.; Shan, W.; Lian, Z.; Liu, J.; He, H. The Smart Surface Modification of Fe_2O_3 by WO_x for Significantly Promoting the Selective Catalytic Reduction of NO_x with NH_3. *APPL CATAL B-ENVIRON.* **2018**, *230*, 165−176.
(25) Wang, H.; Qu, Z.; Dong, S.; Xie, H.; Tang, C. Superior Performance of $Fe_{1-x}W_xO_\delta$ for the Selective Catalytic Reduction of NO_x with NH_3: Interaction between Fe and W. *ENVIRON SCI TECHNOL.* **2016**, *50* (24), 13511−13519.
(26) Geng, Y.; Shan, W.; Yang, S.; Liu, F. W-Modified Mn-Ti Mixed Oxide Catalyst for the Selective Catalytic Reduction of NO with NH_3. *Ind. Eng. Chem. Res.* **2018**, *57* (28), 9112−9119.
(27) Gu, Z.; Cheng, L.; Tan, C.; Sin, S.; Huang, C.; Tang, C. Enriching SO_4^{2-} Immobilization on α-Fe_2O_3 via Spatial Confinement for Robust NH_3-SCR Denitration. *CATALYSTS.* **2022**, *12* (9), 991.
(28) Yang, Z.; Song, J.; Zhang, G.; Sun, X.; Cheng, S.; Zhang, X.; Jiang, Y. Unraveling the Promotion for SO_2 and H_2O Resistance of Transition Metal-Doped CeO_2-TiO_2 Catalysts in NH_3-SCR Reaction: A DFT Study. *J. Hazard. Mater.* **2025**, *489*, No. 137563.
(29) Nie, Y.; Yan, Q.; Chen, S.; O'Hare, D.; Wang, Q. CuTi LDH Derived NH_3-SCR Catalysts with Highly Dispersed CuO Active Phase and Improved SO_2 Resistance. *Catal. Commun.* **2017**, *97*, 47−50.
(30) Cai, Y.; Zhang, B.; Yu, H.; Ji, X.; Sun, J.; Wang, X.; Qian, Q.; Li, L.; Liu, A.; Tan, W.; Gao, F.; Dong, L. Shielding Ceria Based Catalysts from SO_2 Poisoning in NH_3-SCR Reaction: Modification Effect of Acid Metal Oxides. *APPL CATAL B-ENVIRON.* **2024**, *342*, No. 123424.
(31) Guo, S.; Wang, H.; Yang, W.; Fida, H.; You, L.; Zhou, K. Scalable Synthesis of Ca-Doped α-Fe_2O_3 with Abundant Oxygen Vacancies for Enhanced Degradation of Organic Pollutants through Peroxymonosulfate Activation. *APPL CATAL B-ENVIRON.* **2020**, *262*, No. 118250.
(32) Wang, H.; Xu, X.; Yin, L.; Ning, P.; Chen, J.; Cao, J.; Zhang, Q.; Xie, H. SO_2-Induced Dual Active Sites Formation over VO_x/Fe_2O_3 for Accelerating NH_3 Selective Catalytic Reduction of NO_x. *Chem. Eng. J.* **2023**, *462*, No. 142326.
(33) Chen, J.; Guo, L.; Zhu, H.; Qiu, Y.; Yin, D.; Zhang, T.; Chen, J.; Peng, Y.; Li, J. Balancing Redox and Acidic Properties for Optimizing Catalytic Performance of SCR Catalysts: A Case Study of Nanopolyhedron CeO_x-Supported WO_x. *J. Environ. Chem. Eng.* **2021**, *9* (5), No. 105828.
(34) Peng, Y.; Li, K.; Li, J. Identification of the Active Sites on CeO_2-WO_3 Catalysts for SCR of NO_x with NH_3: An In Situ IR and Raman Spectroscopy Study. *APPL CATAL B-ENVIRON.* **2013**, *140*−*141*, 483−492.
(35) Wang, H.; Guo, Y.; Chang, C.; Zhu, X.; Liu, X.; Han, J.; Ge, Q. Enhancing Tungsten Oxide/SBA-15 Catalysts for Hydrolysis of Cellobiose through Doping ZrO_2. *APPL CATAL A-GEN.* **2016**, *523*, 182−192.
(36) Wang, Z.; Niu, Z.; Hao, Q.; Ban, L.; Li, H.; Zhao, Y.; Jiang, Z. Enhancing the Ethynylation Performance of CuO-Bi_2O_3 Nanocatalysts by Tuning Cu-Bi Interactions and Phase Structures. *CATALYSTS.* **2019**, *9* (1), 35.
(37) Gu, Z.; Tan, C.; Zhu, B.; Sin, S.; Ji, J.; Wang, Y.; Cheng, L.; Song, W.; Huang, C.; Tao, M.; Tang, C. SO_4^{2-} Immobilization Regulated by Reaction Atmosphere over ABS Poisoned α-Fe_2O_3 Catalysts for Efficient NO_x Removal. *Chem. Eng. J.* **2023**, *475*, No. 146336.
(38) Wang, H.; Jin, B.; Wang, H.; Ma, N.; Liu, W.; Weng, D.; Wu, X.; Liu, S. Study of Ag Promoted Fe_2O_3@CeO_2 as Superior Soot Oxidation Catalysts: The Role of Fe_2O_3 Crystal Plane and Tandem Oxygen Delivery. *APPL CATAL B-ENVIRON.* **2018**, *237*, 251−262.
(39) Lai, J.-A.; Zhang, Z.; Yang, X.; Zhang, Y. Opening the Black Box: Insights into the Restructuring Mechanism to Steer Catalytic Performance. *Innov. Mater.* **2023**, *1* (2), No. 100020.
(40) Xue, Y.; Liang, J.; Gu, J.-N.; Yu, C.; Guo, M.; Li, K.; Jia, J.; Sun, T. High-Efficient Removal of Oxygen (O_2) Impurity from Hydrogen (H_2) Flow on Nickel-Based Oxide: Effect of Metal Dopants. *Surf. Interface* **2024**, *51*, No. 104664.
(41) Chen, Y.; Li, J.; Teng, W.; Liu, W.; Ren, S.; Yang, J.; Liu, Q. Revealing the Crystal-Plane Effects of CuO During the NH_3-SCR over CuO/TiO_2 Catalysts. *J. Environ. Chem. Eng.* **2023**, *11* (5), No. 110787.
(42) Liu, S.; Liu, J.; Lin, Q.; Xu, S.; Wang, J.; Xu, H.; Chen, Y. Solvent Effects on the Low-Temperature NH_3-SCR Activity and Hydrothermal Stability of WO_3/SiO_2@$CeZrO_x$ Catalyst. *ACS SUSTAIN CHEM ENG.* **2020**, *8* (35), 13418−13429.
(43) Xie, S.; Tan, W.; Li, Y.; Ma, L.; Ehrlich, S. N.; Deng, J.; Xu, P.; Gao, F.; Dong, L.; Liu, F. Copper Single Atom-Triggered Niobia-Ceria Catalyst for Efficient Low-Temperature Reduction of Nitrogen Oxides. *ACS Catal.* **2022**, *12* (4), 2441−2453.
(44) Indovina, V.; Pietrogiacomi, D.; Campa, M. C. CuO_x/Sulphated-ZrO_2, In Situ Sulphated-CuO_x/ZrO_2, and $CuSO_4$/ZrO_2 as Catalysts for the Abatement of NO with C_3H_6 in the Presence of Excess O_2. *APPL CATAL B-ENVIRON.* **2002**, *39* (2), 115−124.
(45) Wang, W.-W.; Yu, W.-Z.; Du, P.-P.; Xu, H.; Jin, Z.; Si, R.; Ma, C.; Shi, S.; Jia, C.-J.; Yan, C.-H. Crystal Plane Effect of Ceria on Supported Copper Oxide Cluster Catalyst for CO Oxidation: Importance of Metal-Support Interaction. *ACS Catal.* **2017**, *7* (2), 1313−1329.
(46) Xu, L.-Y.; Zhou, Q.; Wen, C.-H.; Xu, H.-H.; Zhao, X.; Liu, F.-D.; Luo, M.-F.; Chen, J. Mechanistic Understanding of Oxygen Spillover Enables Efficient Propane Combustion over Pt/$AlSO_x$ Catalyst. *Sep. Purif. Technol.* **2025**, *354*, No. 129193.
(47) Jin, K.; Li, B.; Wang, K.; Luo, H.; Gong, Z.; Wu, W. Reaction Mechanism of NH_3-SCR Denitrification over Rare-Earth Concentrate. *Res. Chem. Intermed.* **2018**, *44* (11), 6933−6943.
(48) An, D.; Yang, Y.; Zou, W.; Cai, Y.; Tong, Q.; Sun, J.; Dong, L. Insight into the Promotional Mechanism of Cu Modification Towards Wide-Temperature NH_3-SCR Performance of NbCe Catalyst. *Chin. J. Chem. Eng.* **2022**, *50*, 301−309.
(49) Chen, L.; Li, J.; Ge, M. DRIFT Study on Cerium-Tungsten/Titiania Catalyst for Selective Catalytic Reduction of NO_x with NH_3. *ENVIRON SCI TECHNOL.* **2010**, *44* (24), 9590−9596.
(50) Liu, Z.; Liu, Y.; Chen, B.; Zhu, T.; Ma, L. Novel Fe-Ce-Ti Catalyst with Remarkable Performance for the Selective Catalytic Reduction of NO_x by NH_3. *Catal. Sci. Technol.* **2016**, *6* (17), 6688−6696.
(51) Urán, L.; Gallego, J.; Ruiz, W.; Bailón-García, E.; Bueno-López, A.; Santamaría, A. Monitoring Intermediate Species Formation by DRIFT during the Simultaneous Removal of Soot and NO_x over $LaAgMnO_3$ Catalyst. *APPL CATAL A-GEN.* **2019**, *588*, No. 117280.

https://doi.org/10.1021/acs.inorgchem.5c01039
Inorg. Chem. 2025, 64, 9798−9806